25. Nguyen M, Camenisch T, Snouwaert JN, Hicks E, Coffman TM, Anderson PA, Malouf NN, Koller BH. The prostaglandin receptor EP4 triggers remodelling of the cardiovascular system at birth. *Nature*. 1997;390:78–81.
26. Nakamura T, Lozano PR, Ikeda Y, Iwanaga Y, Hinek A, Minamisawa S, Cheng CF, Kobuke K, Dalton N, Takada Y, Tashiro K, Ross J Jr, Honjo T, Chien KR. Fibulin-5/DANCE is essential for elastogenesis in vivo. *Nature*. 2002;415:171–175.
27. Rodríguez C, Martínez-González J, Raposo B, Alcudia JF, Guadall A, Badimon L. Regulation of lysyl oxidase in vascular cells: lysyl oxidase as a new player in cardiovascular diseases. *Cardiovasc Res*. 2008;79:7–13.
28. Mäki JM, Räsänen J, Tikkanen H, Sormunen R, Mäkikallio K, Kivirikko KI, Soininen R. Inactivation of the lysyl oxidase gene Lox leads to aortic aneurysms, cardiovascular dysfunction, and perinatal death in mice. *Circulation*. 2002;106:2503–2509.
29. Elzenga NJ, Gittenberger-de Groot AC. Localised coarctation of the aorta. An age dependent spectrum. *Br Heart J*. 1983;49:317–323.
30. Jimenez M, Daret D, Choussat A, Bonnet J. Immunohistological and ultrastructural analysis of the intimal thickening in coarctation of human aorta. *Cardiovasc Res*. 1999;41:737–745.
31. Kim JI, Lakshmikanthan V, Frilot N, Daaka Y. Prostaglandin E2 promotes lung cancer cell migration via EP4-betaArrestin1-c-Src signalsome. *Mol Cancer Res*. 2010;8:569–577.
32. Buchanan FG, Gorden DL, Matta P, Shi Q, Matrisian LM, DuBois RN. Role of beta-arrestin 1 in the metastatic progression of colorectal cancer. *Proc Natl Acad Sci USA*. 2006;103:1492–1497.
33. Wang J, Yin G, Menon P, Pang J, Smolock EM, Yan C, Berk BC. Phosphorylation of G protein-coupled receptor kinase 2-interacting protein 1 tyrosine 392 is required for phospholipase C-gamma activation and podosome formation in vascular smooth muscle cells. *Arterioscler Thromb Vasc Biol*. 2010;30:1976–1982.
34. Mazharian A, Thomas SG, Dhanjal TS, Buckley CD, Watson SP. Critical role of Src-Syk-PLC{gamma}2 signaling in megakaryocyte migration and thrombopoiesis. *Blood*. 2010;116:793–800.
35. Min C, Kirsch KH, Zhao Y, Jeay S, Palamakumbura AH, Trackman PC, Sonenshein GE. The tumor suppressor activity of the lysyl oxidase propeptide reverses the invasive phenotype of Her-2/neu-driven breast cancer. *Cancer Res*. 2007;67:1105–1112.
36. Regan JW. EP2 and EP4 prostanoid receptor signaling. *Life Sci*. 2003;74:143–153.
37. Ma YC, Huang J, Ali S, Lowry W, Huang XY. Src tyrosine kinase is a novel direct effector of G proteins. *Cell*. 2000;102:635–646.
38. Kagan HM, Li W. Lysyl oxidase: properties, specificity, and biological roles inside and outside of the cell. *J Cell Biochem*. 2003;88:660–672.
39. Mäki JM, Sormunen R, Lippo S, Kaarteenaho-Wiik R, Soininen R, Myllyharju J. Lysyl oxidase is essential for normal development and function of the respiratory system and for the integrity of elastic and collagen fibers in various tissues. *Am J Pathol*. 2005;167:927–936.
40. Yoshimura K, Aoki H, Ikeda Y, Fujii K, Akiyama N, Furutani A, Hoshii Y, Tanaka N, Ricci R, Ishihara T, Esato K, Hamano K, Matsuzaki M. Regression of abdominal aortic aneurysm by inhibition of c-Jun N-terminal kinase. *Nat Med*. 2005;11:1330–1338.
41. Smith-Mungo LI, Kagan HM. Lysyl oxidase: properties, regulation and multiple functions in biology. *Matrix Biol*. 1998;16:387–398.
42. Rodríguez C, Alcudia JF, Martínez-González J, Raposo B, Navarro MA, Badimon L. Lysyl oxidase (LOX) down-regulation by TNFalpha: a new mechanism underlying TNFalpha-induced endothelial dysfunction. *Atherosclerosis*. 2008;196:558–564.
43. Rodríguez C, Raposo B, Martínez-González J, Casaní L, Badimon L. Low density lipoproteins downregulate lysyl oxidase in vascular endothelial cells and the arterial wall. *Arterioscler Thromb Vasc Biol*. 2002;22:1409–1414.
44. Song YL, Ford JW, Gordon D, Shanley CJ. Regulation of lysyl oxidase by interferon-gamma in rat aortic smooth muscle cells. *Arterioscler Thromb Vasc Biol*. 2000;20:982–988.
45. Peng C, Yan S, Ye J, Shen L, Xu T, Tao W. Vps18 deficiency inhibits dendritogenesis in Purkinje cells by blocking the lysosomal degradation of Lysyl Oxidase. *Biochem Biophys Res Commun*. 2012;423:715–720.
46. Zhu L, Dagher E, Johnson DJ, Bedell-Hogan D, Keeley FW, Kagan HM, Rabinovitch M. A developmentally regulated program restricting insolubilization of elastin and formation of laminae in the fetal lamb ductus arteriosus. *Lab Invest*. 1993;68:321–331.
47. Nakashima Y, Sueishi K. Alteration of elastic architecture in the lathyritic rat aorta implies the pathogenesis of aortic dissecting aneurysm. *Am J Pathol*. 1992;140:959–969.
48. Sibon I, Sommer P, Lamaziere JM, Bonnet J. Lysyl oxidase deficiency: a new cause of human arterial dissection. *Heart*. 2005;91:e33.
49. Yokoyama U, Ishiwata R, Jin MH, Kato Y, Suzuki O, Jin H, Ichikawa Y, Kumagaya S, Katayama Y, Fujita T, Okumura S, Sato M, Sugimoto Y, Aoki H, Suzuki S, Masuda M, Minamisawa S, Ishikawa Y. Inhibition of EP4 signaling attenuates aortic aneurysm formation. *PLoS ONE*. 2012;7:e36724.

CLINICAL PERSPECTIVE

The ductus arteriosus (DA) is a fetal bypass artery between the aorta and the pulmonary artery. Although the DA closes immediately after birth, it remains open in some infants, a condition known as patent DA. Patent DA remains a frequent problem among premature infants with significant morbidity and mortality. Both vascular contraction and remodeling (ie, intimal thickening) are required for complete anatomical closure of the DA. Decreased elastogengesis is known as a hallmark of DA remodeling and is thought to contribute to intimal thickening of the DA. However, the molecular mechanisms of decreased elastogenesis are not fully understood. Herein, we show that prostaglandin E_2 (PGE_2) receptor EP4 signaling promotes degradation of the mature lysyl oxidase protein, a cross-linking enzyme for elastic fibers, only in the DA, leading to decreased elastogenesis. The newly recognized PGE-EP4-c-Src-PLCγ-signaling pathway most likely contributes to the lysosomal degradation of lysyl oxidase. Based on these data, it appears that PGE-EP4 signaling is required for DA remodeling and that inhibition of this signaling by cyclooxygenase inhibitors may attenuate DA remodeling after birth, especially in premature infants in which the DA is not fully remodeled. Activation of the c-Src-PLCγ signaling pathway may be an additional strategy to promote anatomical closure of the immature DA.

SUPPLEMENTAL MATERIAL

Supplemental Methods

Reagents

8-p-Methoxyphenylthon-2-Omethyl-cAMP (pMe-cAMP) and N6-benzoyladenosine-cAMP (Bnz-cAMP) were purchased from BioLog Life Science Institute (Bremen, Germany) and Sigma (St. Louis, MO), respectively. PGE_2, sulprostone, butaplost, gallein, BAPN, bisindolylmaleimide (bis), U73122, U0126, LY294002, PAO, EIPA, and 8-Bromo-cAMP (Br-cAMP) were purchased from Sigma-Aldrich (St. Louis, MO). CPZ, MβCD, MG132, and NH_4Cl were obtained from Wako (Osaka, Japan). The PKA inhibitor (14–22), bafilomycin A1, PP2, and m-3M3FBS were obtained from Calbiochem (Darmstadt, Germany). ONO-AE1-329 was kindly provided by ONO Pharmaceutical Company (Osaka, Japan). Antibodies for LOX and pro-LOX for immunoblotting were obtained from Abcam (Cambridge, UK) and Novus Biological (Littleton, CO), respectively. Anti-LOX antibody for immunohistochemistry and anti-BMP-1 were obtained from US Biological (Swampscott, MA) and Santa Cruz Biotechnology (Santa Cruz, CA), respectively. Anti-elastin and anti-EP4 antibodies were obtained from Elastin Products Company (Owensville, MO) and Caymanchemical (Ann Arbor, MI), respectively. Anti-PLCγ and anti-phosphorylated PLCγ antibodies were obtained from Cell Signaling (Beverly, MA). Anti-MMP-2 and anti-MMP-9 antibodies were from R&D Systems (Minneapolis, MN). Anti-fibrillin-1 antibody was kindly

provided from Dr. Nakamura (Kansai University, Japan).

Isolation and culture of rat smooth muscle cells (SMCs)

Vascular SMCs were obtained from the DA and aorta of Wistar rat fetuses on the 21st day of gestation (SLC Inc.) as previously described[1]. Using the same protocol, pulmonary SMCs were isolated from the branch extralobular pulmonary arteries from Wistar rats on the 21st day of gestation. SMCs were used at passages 4 to 6.

Immunoblot analysis

Proteins from whole cells were analyzed by immunoblotting as previously described [1].

Adenovirus construction

Adenovirus of EP4 was kindly provided from Dr. Y. Kobayashi (Matsumoto Dental University, Japan)[2]. A control adenovirus vector with LacZ was used at the same multiplicity of infection.

RNA interference (siRNA)

Double-stranded siRNAs to the selected regions of EP4 (stealth RNAi RSS331316) and the negative siRNA purchased from Invitrogen (San Diego, CA). According to the manufacturer's instructions, cells were transfected with siRNA (300 pmol), using Lipofectamin RNAiMAX (Invitrogen).

Quantitative and semi-quantitative reverse transcriptase-polymerase chain reaction (RT-PCR)

Isolation of total RNA and generation of cDNA were performed and RT-PCR analysis was done

as previously described [1]. The primers were designed based on the rat nucleotide sequences of EP4 (5'-CTC GTG GTG CGA GTG TTC AT-3' and 5'-AAG CAA TTC TGA TGG CCT GC-3') and BMP-1 (5'-CAT CTC CAT CGG CAA GAA C-3' and 5'-CTC GAC TTC CTG AAC TTC CAT C-3'). Each primer set was designed between multiple exons. The abundance of each gene was determined relative to the 18S transcript.

Electron microscopy

Electron microscopic analysis for elastic fiber formation was performed as previously described [3].

Gelatin zymography

MMP activity was examined by gelatin zymography as previously described [4].

In situ hybridization

Expression of EP4 mRNA in mice fetuses on day 12.5, 16.5, and 18.5 of gestation was evaluated by *in situ* hybridization. A 543 bp DNA fragment corresponding to nucleotide positions 1373 to 1915 of mouse EP4 cDNA (Gen-Bank NM_008965) was cloned into pGEMT-Easy vector (Promega, Madison, WI) and used for the generation of sense and antisense RNA probes. Digoxigenin-labeled RNA probes were prepared with DIG RNA Labeling Mix (Roche, Basel, Switzerland). Hybridization was performed with probes at concentrations of 300 ng/ml in the Probe Diluent-1 (Genostaff, Tokyo, Japan) at 60°C for 16 h. After treatment with 0.5% blocking reagent (Roche) in TBST for 30 min, the sections were incubated with anti-DIG AP conjugate (Roche) diluted 1:1000 with TBST for 2 hr at room temperature (RT). Coloring reactions were

performed with NBT/BCIP solution overnight and then washed with PBS. The sections were counterstained with Kernechtrot stain solution (Muto Pure Chemicals, Tokyo, Japan), and mounted with CC/Mount (DBS).

Supplemental Table 1.

Summary of patient profile

Case	Age at Operation	Diagnosis
1	2 days	CoA, VSD
2	3 days	TGA, CoA
3	4 days	CoA, VSD
4	4 days	CoA, VSD
5	13 days	CoA, VSD
6	13 days	CoA, VSD
7	1 month	hypoLV, CoA, VSD

CoA: Coarctation of the Aorta, VSD: Ventricular Septum Defect,

TGA: Transposition of the Great Arteries, hypoLV: hypoplastic Left Ventricule.

Supplemental table 2.

Correlation between elastic fiber formation and expression of EP4 and LOX

	Elastic fiber formation - EP4			Elastic fiber formation - LOX			EP4 - LOX		
case	r	n	*p* value	r	n	*p* value	r	n	*p* value
1	-0.7164	68	< 0.0001***	0.8095	68	< 0.0001***	-0.6723	68	< 0.0001***
2	-0.8277	22	< 0.0001***	0.6043	22	0.0029**	-0.6101	22	0.0026**
3	-0.8869	44	< 0.0001***	0.6431	44	< 0.0001***	-0.5626	44	< 0.0001***
4	-0.7116	62	< 0.0001***	0.765	62	< 0.0001***	-0.4875	62	< 0.0001***
5	-0.547	35	0.0007***	0.7561	35	< 0.0001***	-0.5335	35	0.001***
6	-0.523	28	0.0043**	0.6032	28	0.0007***	-0.6066	28	0.0006***
7	-0.7851	19	< 0.0001***	0.8649	19	< 0.0001***	-0.5765	19	0.0098**

r: correlation coefficient; n: number of sampling points. *, $p < 0.05$; **, $p < 0.01$; ***, $p < 0.001$

Supplemental Figure 1

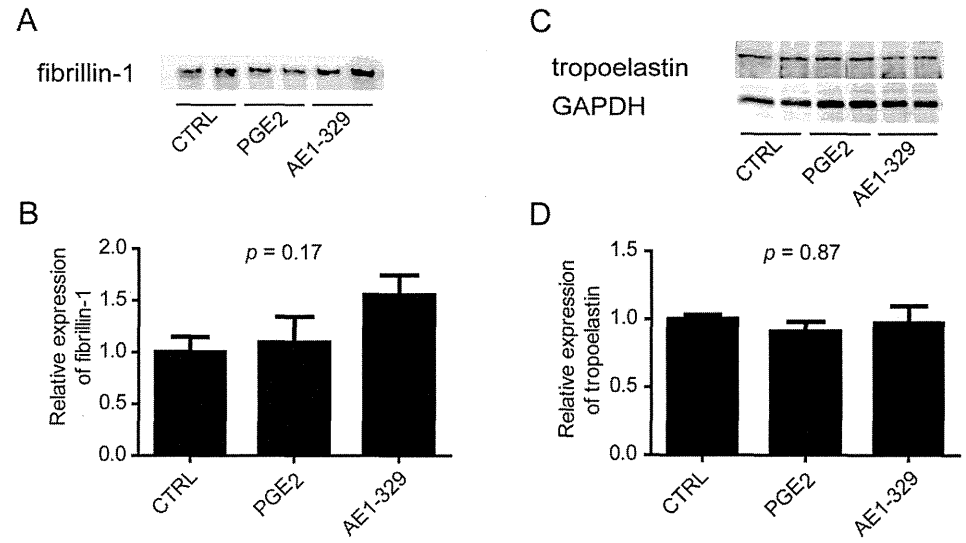

Supplemental Figure 2

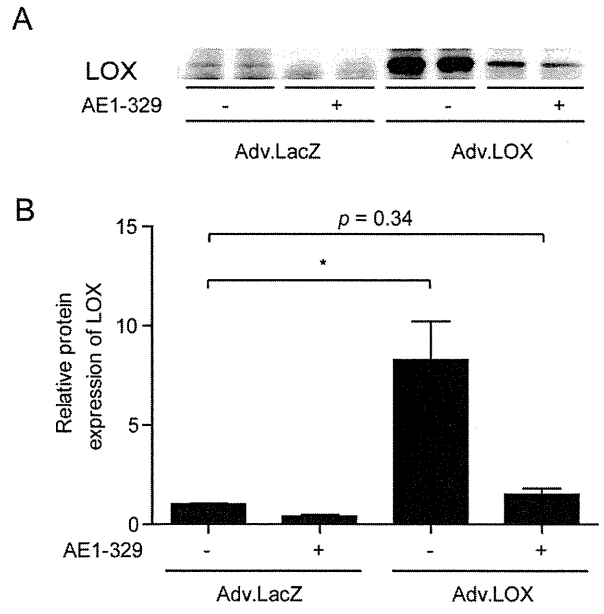

Supplemental Figure 3

A

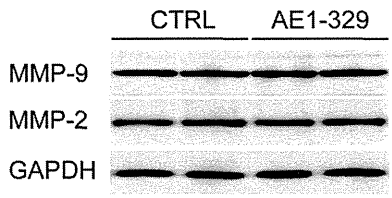

B

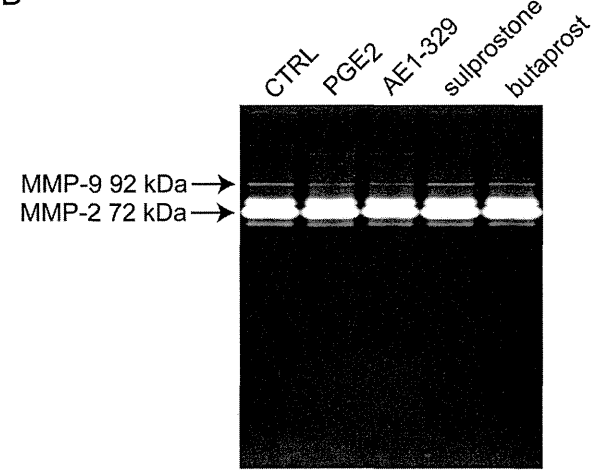

C

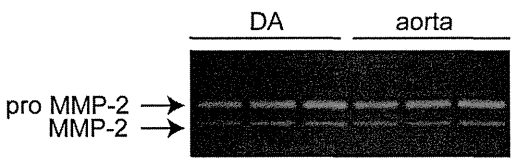

Supplemental Figure 4

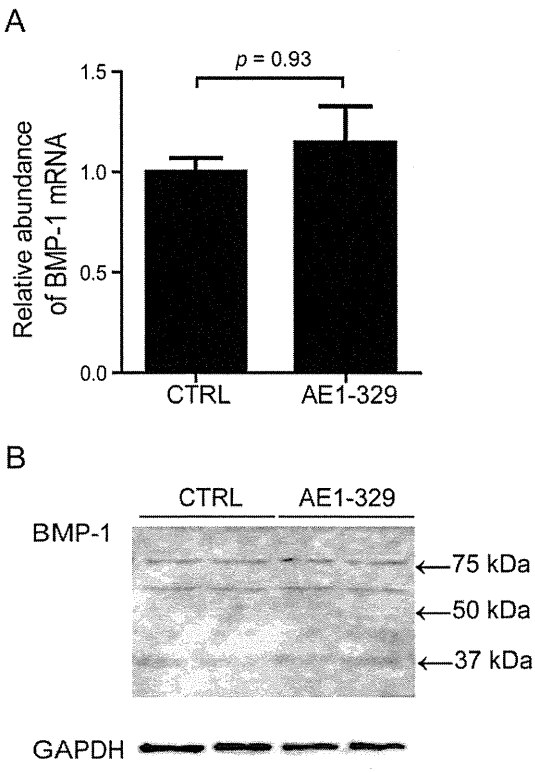

Supplemental Figure 5

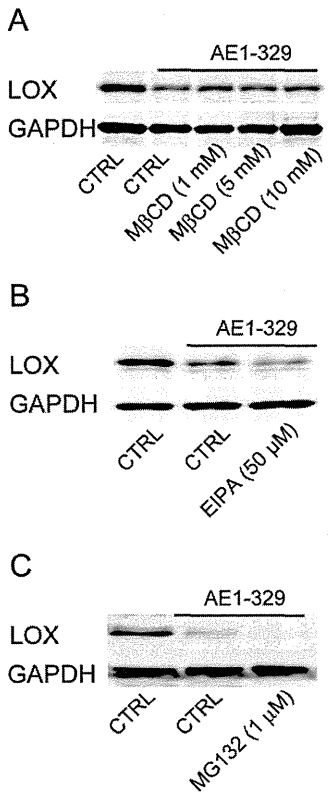

Supplemental Figure Legends

Supplemental Figure 1

EP4 signaling did not affect protein expression of tropoelastin and fibrillin-1.

(A) Protein expression of fibrillin-1 in culture medium of DASMCs treated with either PBS, PGE_2 (1 μM), or AE-329 (1 μM) for 72 h. (B) Quantification of (A), n = 4. (C) Protein expression of tropoelastin in whole cell lysate of DASMCs treated with either PBS, PGE_2 (1 μM), or AE-329 (1 μM) for 72 h. (D) Quantification of (C), n = 4.

Supplemental Figure 2

Overexpression of LOX protein in DASMCs transfected with Adv.LOX.

(A) Protein expression of LOX in culture medium of DASMCs transfected Adv.LacZ or Adv.LOX in the presence or absence of AE-329 (1 μM). The time-course of transfection and drug administration was same as Figure 4I. (B) Quantification of (A), n = 4, $*p < 0.05$.

Supplemental Figure 3

EP4 signaling did not affect expression or activation of MMP-2 or -9 in DASMCs.

(A) Protein expression of MMP-2 and-9 in DASMCs treated with or without AE1-329 (1 μM) for 72 h. (B) Gelatin zymography of DASMCs treated with 1 μM of PGE2 or each EP agonist. (C) Gelatin zymography of the rat DA and aorta on the 21st day of gestation.

Supplemental Figure 4

EP4 signaling did not change BMP-1 expression in DASMCs.

(A) Expression of BMP-1 mRNA in DASMCs treated with or without AE1-329 (1 μM) for 24 h. n = 4. (B) Representative image of protein expression of BMP-1 in DASMCs treated with or without AE1-329 (1 μM) for 72 h.

Supplemental Figure 5

LOX degradation was associated with caveolar endocytosis, macropinocytosis, and proteosome.

(A) Representative figures of protein expression of LOX in whole cell lysate of DASMCs treated with MbCD, EIPA, or MG132 in the presence of AE1-329 (1 μM).

References

1. Yokoyama U, Minamisawa S, Adachi-Akahane S, Akaike T, Naguro I, Funakoshi K, Iwamoto M, Nakagome M, Uemura N, Hori H, Yokota S, Ishikawa Y. Multiple transcripts of ca2+ channel alpha1-subunits and a novel spliced variant of the alpha1c-subunit in rat ductus arteriosus. *Am J Physiol Heart Circ Physiol*. 2006;290:H1660-1670

2. Kobayashi Y, Take I, Yamashita T, Mizoguchi T, Ninomiya T, Hattori T, Kurihara S, Ozawa H, Udagawa N, Takahashi N. Prostaglandin e2 receptors ep2 and ep4 are down-regulated during differentiation of mouse osteoclasts from their precursors. *J Biol Chem*. 2005;280:24035-24042

3. Nakamura T, Lozano PR, Ikeda Y, Iwanaga Y, Hinek A, Minamisawa S, Cheng CF, Kobuke K, Dalton N, Takada Y, Tashiro K, Ross Jr J, Honjo T, Chien KR. Fibulin-5/dance is essential for elastogenesis in vivo. *Nature*. 2002;415:171-175

4. Yoshimura K, Aoki H, Ikeda Y, Fujii K, Akiyama N, Furutani A, Hoshii Y, Tanaka N, Ricci R, Ishihara T, Esato K, Hamano K, Matsuzaki M. Regression of abdominal aortic aneurysm by inhibition of c-jun n-terminal kinase. *Nat Med*. 2005;11:1330-1338

Atherosclerosis 233 (2014) 590–600

Contents lists available at ScienceDirect

Atherosclerosis

journal homepage: www.elsevier.com/locate/atherosclerosis

Three-dimensional multilayers of smooth muscle cells as a new experimental model for vascular elastic fiber formation studies

Ryo Ishiwata [a], Utako Yokoyama [a,*], Michiya Matsusaki [b], Yoshiya Asano [c], Koji Kadowaki [b], Yasuhiro Ichikawa [a], Masanari Umemura [a], Takayuki Fujita [a], Susumu Minamisawa [d], Hiroshi Shimoda [c], Mitsuru Akashi [b], Yoshihiro Ishikawa [a,*]

[a] Cardiovascular Research Institute, Yokohama City University Graduate School of Medicine, 3-9 Fukuura, Kanazawa-ku, Yokohama, Kanagawa 236-0004, Japan
[b] Department of Applied Chemistry, Graduate School of Engineering, Osaka University, Osaka, Japan
[c] Department of Neuroanatomy, Cell Biology and Histology, Hirosaki University Graduate School of Medicine, Hirosaki, Japan
[d] Department of Cell Physiology, Jikei University School of Medicine, Tokyo, Japan

ARTICLE INFO

Article history:
Received 9 August 2013
Received in revised form
20 January 2014
Accepted 21 January 2014
Available online 29 January 2014

Keywords:
Blood vessels
Smooth muscle cells
Elastic fibers
Nanotechnology
Tissue engineering
Fibronectin

ABSTRACT

Objective: Elastic fiber formation is disrupted with age and by health conditions including aneurysms and atherosclerosis. Despite considerable progress in the understanding of elastogenesis using the planar culture system and genetically modified animals, it remains difficult to restore elastic fibers in diseased vessels. To further study the molecular mechanisms, in vitro three-dimensional vascular constructs need to be established. We previously fabricated vascular smooth muscle cells (SMCs) into three-dimensional cellular multilayers (3DCMs) using a hierarchical cell manipulation technique, in which cells were coated with fibronectin-gelatin nanofilms to provide adhesive nano-scaffolds. Since fibronectin is known to assemble and activate elastic fiber-related molecules, we further optimized culture conditions.
Methods and results: Elastica stain, immunofluorescence, and electron microscopic analysis demonstrated that 3DCMs, which consisted of seven layers of neonatal rat aortic SMCs cultured in 1% fetal bovine serum (FBS) in Dulbecco's modified Eagle's medium, exhibited layered elastic fibers within seven days of being in a static culture condition. In contrast, the application of adult SMCs, 10% FBS, ε-poly(-lysine) as an alternative adhesive for fibronectin, or four-layered SMCs, failed to generate layered elastic fiber formation. Radioimmunoassay using [^{3}H]valine further confirmed the greater amount of cross-linked elastic fibers in 3DCMs than in monolayered SMCs. Layered elastic fiber formation in 3DCMs was inhibited by the lysyl oxidase inhibitor β-aminopropionitrile, or prostaglandin E_2. Furthermore, infiltration of THP-1-derived macrophages decreased the surrounding elastic fiber formation in 3DCMs.
Conclusion: 3DCMs may offer a new experimental vascular model to explore pharmacological therapeutic strategies for disordered elastic fiber homeostasis.

1. Introduction

Arterial walls have a highly organized layer structure that consists of various cells and extracellular matrix (ECM) components. In particular, the vascular media is composed of a dense population of concentrically organized smooth muscle cells (SMCs) and elastic fibers, and plays a pivotal role in maintaining sufficient blood pressure, even during variations in hemodynamic stress. In physiological conditions, SMCs synthesize elastin and other specific molecules, which are incorporated into elastic fibers and arranged into concentric rings of elastic lamellae around the arterial media [1]. In contrast, arterial compliance and distensibility are impaired in the presence of cardiovascular disease and risk factors such as aortic aneurysm, atherosclerosis, ischemic heart disease, aging, hypertension, cigarette smoking, and diabetes [2]. Hence, impaired elastic properties are associated with arterial dysfunction and pathophysiology [2,3].

Changes in arterial elastic properties are the result of alterations in the intrinsic structural properties of the artery, including the fracturing and thinning of elastic fibers. Current approaches to

* Corresponding authors. Tel.: +81 45 787 2575; fax: +81 45 787 1470.
E-mail addresses: utako@yokohama-cu.ac.jp, CZL03430@nifty.com (U. Yokoyama), yishikaw@med.yokohama-cu.ac.jp (Y. Ishikawa).

0021-9150/$ – see front matter © 2014 Elsevier Ireland Ltd. All rights reserved.
http://dx.doi.org/10.1016/j.atherosclerosis.2014.01.045

examining the elastogenesis and degradation of elastic fibers rely heavily on the use of the planar culture of vascular SMCs and genetically modified animals. These approaches have been instrumental in numerous discoveries and have been modified to create very elegant experimental designs [1,4–7]. Currently, however, no pharmacological strategy to promote elastogenesis and prevent the degradation of elastic fiber formation is available, and the molecular mechanisms of the regulation of elastic fiber formation remain to be studied. The two-dimensional (2D) monolayer culture system is a useful method for isolating specific factors and their effects on specific cell types [5–7], but it lacks the native-like layered structure of elastic fibers. Therefore, changes in the spatial arrangement of elastic fibers induced by various stimuli and the infiltration of immune cells cannot be observed. In-vivo analysis, on the other hand, often fails to discriminate among the various and complex factors. In this context, in vitro reconstruction vessel models overcoming these limitations are considered potential platforms of vascular biology that can provide further insights into the spatio-temporal molecular mechanisms of elastic fiber formation.

We previously developed a novel three-dimensional (3D) cell construction method [8] and created 3D-layered blood vessel constructs consisting of human umbilical arterial SMCs and human umbilical vascular endothelial cells [9]. To develop the 3D-cellular multilayers (3DCMs), we fabricated nanometer-sized cell adhesives like ECM scaffolds onto the surface of a cell membrane, which enables another cellular layer to adhere to the coated cell surface. We employed a layer-by-layer (LbL) technique to fabricate fibronectin–gelatin nanofilms onto living cell membranes, because the LbL technique produces nanometer-sized polymer films with a controllable nanometer thickness through the alternate immersion into interactive polymer solutions. We found that approximately 6 nm of fibronectin-based nanofilms were suitable for developing stable adhesive scaffolds and for creating allogeneic or xenogeneic multiple cell layers.

In addition to the cell adhesion effect, fibronectin has been known to orchestrate the assembly of the ECM [10–15]. In particular, recent reports suggest that fibronectin fiber assembles pericellularly into fibrillin microfibrils that have a complex structural organization and are widespread in elastic tissues [10,16]. Furthermore, fibronectin binds to lysyl oxidase (LOX), a cross-linking enzyme for elastic fibers, and acts as a scaffold for enzymatically active 30 kDa LOX [14]. Using scanning electron microscopy and transmission electron microscopy, we observed that fibronectin formed extracellular fibrils in the abovementioned 3DCMs within 24 h cultures [9], suggesting that fibronectin-coated SMCs have the potential to produce elastic fiber assemblies. In this context, we aimed to create the first scaffold-free 3D cellular multilayers (3DCMs) that are specifically designed for investigating the spatial regulation of vascular elastic fibers by employing this LbL assembly technique. The present study demonstrates that the optimized culture conditions provided layered elastic fiber formation in the 3DCMs consisting of neonatal rat SMCs within seven days of static culture conditions. In the 3DCMs, it was observed in the vertical view that macrophage infiltration or prostaglandin E_2 (PGE_2) changed the spatial arrangement of elastic fibers.

2. Materials and methods

Expanded materials and methods are described in Supplemental data.

2.1. Animals

Neonate (day 1) and adult Wistar rats (4–5months old) were obtained from Japan SLC, Inc. (Shizuoka, Japan). All animal studies were approved by the institutional animal care and use committees of Yokohama City University.

2.2. Cell culture

Vascular SMCs in primary culture were obtained from the aorta of rat neonates (day 1) as previously described [17–19]. Briefly, the minced tissues were digested with a collagenase-dispase enzyme mixture at 37 °C for 20 min. The cell suspensions were then centrifuged, and the medium was changed to a collagenase II enzyme mixture. After 12 min of incubation at 37 °C, cell suspensions were plated on 35 mm poly-L-lysine-coated dishes The growth medium contained Dulbecco's modified Eagle medium (DMEM) with 10% fetal bovine serum (FBS), 100 U/ml penicillin, and 100 mg/ml streptomycin (Invitrogen, Carlsbad, CA). Human adult aortic SMCs were obtained from Lonza (Walkersville, MD, USA). The confluent SMCs were used at passages 5–7. THP-1 cells were obtained from the Health Science Research Resources Bank (Osaka, Japan) and were maintained in RPMI 1640 medium (Wako, Osaka, Japan) supplemented with 10% FBS. All cells were cultured in a moist tissue culture incubator at 37 °C in 5% CO_2-95% ambient mixed air.

2.3. Construction of 3DCMs

Construction of 3DCMs was performed as previously described [8]. Briefly, a cell disk LF (Sumitomo Bakelite, Tochigi, Japan) was rinsed with 50 mM Tris–HCl buffer solution (pH 7.4) for 15 min and coated with fibronectin (0.2 mg/ml) for 30 min at 37 °C. SMCs were cultured on the cell disk (11×10^4 cells/cm^2) and incubated for 12 h in 10% FBS/DMEM. The monolayered SMCs were then immersed alternatively in a solution of fibronectin (0.2 mg/ml) and gelatin (0.2 mg/ml). After nine steps of LbL assembly with fibronectin and gelatin, a second cell layer was seeded on the first cell layer (11×10^4 cells/cm^2) and incubated for 6–12 h at 37 °C. The cycles of LbL nanofilm assembly and subsequent cell seeding were repeated six times in four days to construct seven-layered 3DCMs. During the first four days, the medium was refreshed daily. Twelve hours after the seeding of the last layer, the culture media was changed to DMEM or DMEM/F-12 (Gibco, Carlsbad, CA) containing 1% FBS or 10% FBS. The 3DCMs were incubated for an additional 48 h and either fixed in buffered 10% formalin or harvested in TRIzol (Invitrogen, Carlsbad, CA). The time-course of the 3DCM experiments is shown in Supplemental Fig. 1A. Stimulation by β-aminoproprionitrile (BAPN) or PGE_2 (1 μM) was performed simultaneously with the medium change on day 5. For macrophage infiltration assay, seven-layered 3DCMs at day 5 were put on a 24-well plate and applied with 500 μl of RPMI 1640 medium containing THP-1 cells (2.0×10^5 cells) with or without phorbol 12-myristate 13-acetate (PMA, 0.1 μM). The 3DCMs were incubated for 1 h at 37 °C. Next, unattached THP-1 cells were washed out with PBS and 3DCMs were incubated in 1% FBS/DMEM for 72 h until fixation. Control monolayered neonatal rat aortic SMCs (2D-SMCs) were plated on day 4 in the same density as a single layer in 3DCMs (11×10^4 cells/cm^2), and were incubated for 48 h. Four-layered 3DCMs were constructed from day 3 following the same time-course. The proportional increase in the thickness of 3DCMs with the number of seeding events was shown in Supplemental Fig. 1B. To confirm the effect of fibronectin nanofilms, ε-poly(lysine) (0.2 mg/ml) was used as an alternative adhesive polymer.

2.4. Quantitative measurement of insoluble elastin

Newly synthesized insoluble elastin was measured as previously described [20,21]. Briefly, after the seven-layered 3DCMs and 2D-

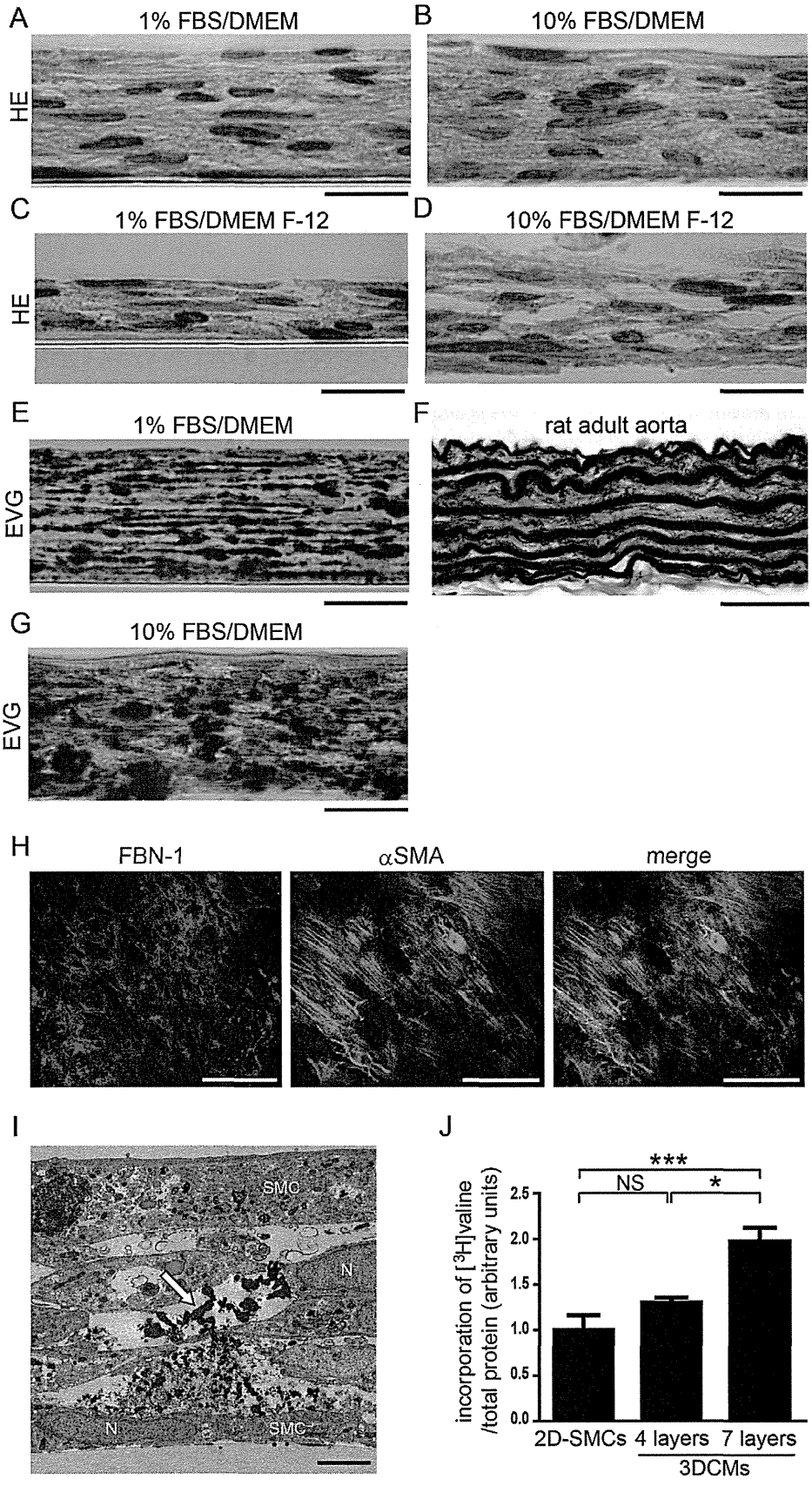
A
1% FBS/DMEM
B
10% FBS/DMEM
HE
C
1% FBS/DMEM F-12
D
10% FBS/DMEM F-12
HE
E
1% FBS/DMEM
F
rat adult aorta
EVG
G
10% FBS/DMEM
EVG
H
FBN-1
αSMA
merge
I
SMC
N
N
SMC
J
***
NS
*
incorporation of [3H]valine /total protein (arbitrary units)
2.5
2.0
1.5
1.0
0.5
0.0
2D-SMCs
4 layers
7 layers
3DCMs

SMCs were constructed for four days and one day, respectively, as mentioned above, they were incubated in 2 ml of 1% FBS/DMEM in the presence of 5 μCi [^{3}H]valine (ART 0466, American Radiolabeled Chemicals, Inc., St. Louis, MO) for an additional three days. One day after the monolayered SMCs were plated, the cells were harvested in 0.1 M acetic acid on ice. After centrifugation, the pellets were boiled in 0.1 N NaOH for 1 h. The NaOH-insoluble fractions were collected by centrifugation and were boiled in 5.7 N HCl for 1 h. The samples mixed with scintillation fluid were measured for radioactivity using a scintillation counter (Beckman Coulter).

2.5. Statistical analyses

Data are presented as the mean ± standard error of the mean (SEM) of independent experiments. Data were analyzed by the unpaired Student's *t*-test or one-way analysis of variance (ANOVA) followed by Newman–Keuls multiple comparison test. $p < 0.05$ was considered significant.

3. Results

3.1. 3DCMs exhibited layered elastic fiber formation

Most of the elastic fiber proteins are expressed in the second half of development and increase throughout the early postnatal period [22]. This is followed by a decrease in expression to low levels that persist through adulthood [23]. Consistent with this in vivo evidence, it has been suggested that neonatal rat SMCs produce a greater amount of elastin and elastic fibers compared to adult rat SMCs [24,25]. We confirmed that mRNA expression levels of elastic fiber–related genes, such as tropoelastin, fibrilin-1, fibulin-4, fibulin-5, LOX, and LOX-like 1, are significantly greater in the neonatal rat aorta (1 day old) than in the adult rat aorta (Supplemental Fig. 2).

On the basis of these data, we used neonatal rat SMCs to fabricate 3DCMs as in vitro vascular constructs. First, we cultured 3DCMs with four different culture media, including DMEM and DMEM F-12, because DMEM F-12 includes proline, one of the major amino acids that constitutes elastin protein, and copper, which enhances LOX activity [26]. Contrary to expectations, nucleus counting using HE stain revealed that viability was better in the 3DCMs cultured in DMEM (Fig. 1A–B, Supplemental Fig. 3) than in DMEM F-12 containing either 10% or 1% FBS (Fig. 1C–D). Next, we compared elastic fiber formation using Elastica van Gieson (EVG) stain in 3DCMs cultured in DMEM containing 10% or 1% FBS. We found that 3DCMs cultured in 1% FBS/DMEM exhibited layered elastic fiber formation (Fig. 1E), although the elastic fiber formation did not reach that observed in adult rat aorta (Fig. 1F) The 3DCMs culture in 10% FBS/DMEM exhibited a certain amount of positive stain of elastic fibers, but no layered elastic fiber formation was clearly detected (Fig. 1G). In the 3DCMs culture in 1% FBS/DMEM, co-immunofluorescence for fibrillin-1 and α-smooth muscle actin (αSMA) demonstrated a fiber meshwork of fibrillin-1 on the SMC surface (Fig. 1H). Electron microscopic analysis also confirmed the presence of elastic laminae between SMC layers (Fig. 1I).

To investigate whether the use of fibronectin nanofilms is required for elastic fiber formation in the 3DCMs, we applied ε-poly(lysine), a synthesized polymer that electrically binds to gelatin, as an alternative to fibronectin in the 3DCMs. We found that ε-poly(lysine) did not provide layered elastic fiber formation (Supplemental Fig. 4A). As expected, the 3DCMs composed of adult human aortic SMCs or adult rat aortic SMCs also did not exhibit elastic fiber formation (Supplemental Fig. 4B–C). Furthermore, we compared elastic fiber formation between the 3DCMs and another 3D model, i.e., the spheroid culture system. We constructed spheroids of neonatal rat SMCs with the same culture conditions of 3DCM construction (Supplemental Fig. 5A) and found that a few elastic laminae were formed in the outer shell of rat SMC spheroids, but not in the porous core (Supplemental Fig. 5B–C).

To quantify the amount of mature (i.e., cross-linked) elastic fibers in 3DCMs, we metabolically labeled newly synthesized elastin with [^{3}H]valine, and measured the incorporation of [^{3}H]valine in the NaOH-insoluble fraction of these cells, which reflects the amount of newly synthesized mature elastic fibers [27]. As shown in Fig. 1J, in 3DCMs cultured with 1% FBS/DMEM, we detected a significant increase in the incorporation of [^{3}H]valine into the insoluble fraction compared to 2D-SMCs cultured in the same culture medium. Interestingly, seven-layered 3DCMs produced a larger amount of cross-linked elastic fibers than four-layered 3DCMs even if the values were compared in the same amount of protein (Fig. 1J and Supplemental Fig. 4D). These data suggest that seven-layered 3DCMs consisting of fibronectin coating neonatal rat aortic SMCs cultured in 1% FBS/DMEM produced layered elastic fibers in vitro.

3.2. Expression of elastic fiber-related genes in 3DCMs

Elastic fibers are complex structures that contain elastin as well as microfibrils and fibulins [1]. Elastin is the major component of mature elastic fibers, and microfibrils, such as fibrillin-1 and fibrillin-2, are known to facilitate elastin assembly and provide overall structure to the growing elastic fiber [1]. Tropoelastin's lysine residues are, in turn, modified to form covalent cross-links between and within elastin molecules by LOX, resulting in the functional form of elastic fibers [1,26]. The deposition of fibulin-5 on microfibrils also promotes the coacervation and alignment of tropoelastins on microfibrils, and facilitates the cross-linking of tropoelastin by tethering LOX–like 1, 2, and 4 enzymes [20]. Fibulin-4 interacts with LOX and recruits LOX to elastin monomers as well [28].

We examined the mRNA expression levels of these genes in the 3DCMs cultured in DMEM containing 1% or 10% FBS and 2D-SMCs. The expression levels of tropoelastin and fibrillin-2 mRNAs were greater in the 3DCMs cultured in 1% FBS/DMEM than in 10% FBS/DMEM (Fig. 2A–B). The expression levels of other genes, including fibrillin-1, fibulin-4, fibulin-5, LOX, and LOX-like 1, were similar among different serum concentrations (Fig. 2C–G). Similar serum withdrawal effects on tropoelastin and fibrillin-2 mRNA were also observed in 2D-SMCs (Supplemental Fig. 6A–B). In 3DCMs cultured in 1% FBS/DMEM, abundant protein expressions of tropoelastin and LOX were also observed (Fig. 2H–I). However, there was no difference in the expression of elastic fiber-related genes between 2D-SMCs and 3DCMs (Fig. 2A–G, J–K). These data

Fig. 1. 3DCMs cultured in 1% FBS/DMEM exhibited layered elastic fibers. (A–B) Hematoxylin eosin (HE) stain of 3DCMs cultured in DMEM containing either 1% (A) or 10% FBS (B). HE stain of 3DCMs cultured in DMEM F-12 containing either 1% (C) or 10% FBS (D). (E) Elastica van Gieson (EVG) stain of 3DCMs cultured in 1% FBS/DMEM. Scale bars: 10 μm. (F) EVG stain of rat adult aorta. Scale bar: 50 μm. (G) EVG stain of 3DCMs cultured in 10% FBS/DMEM. Scale bar: 10 μm. (H) Confocal images of the fibrillin-1 and αSMA immunofluorescence in the 3DCMs cultured in 1% FBS/DMEM. red: fibrillin-1. Green: αSMA. Scale bar: 50 μm. (I) Electron microscopic image of 3DCMs. White arrow indicates elastic fibers. N: nucleus. Scale bar: 2.0 μm. (J) Radioimmunoassay of elastogenesis in 2D-SMCs, four-layered 3DCMs, and seven-layered 3DCMs cultured in 1% FBS/DMEM. $n = 4–8$. $^*p < 0.05$; $^{***}p < 0.001$; NS: not significant.

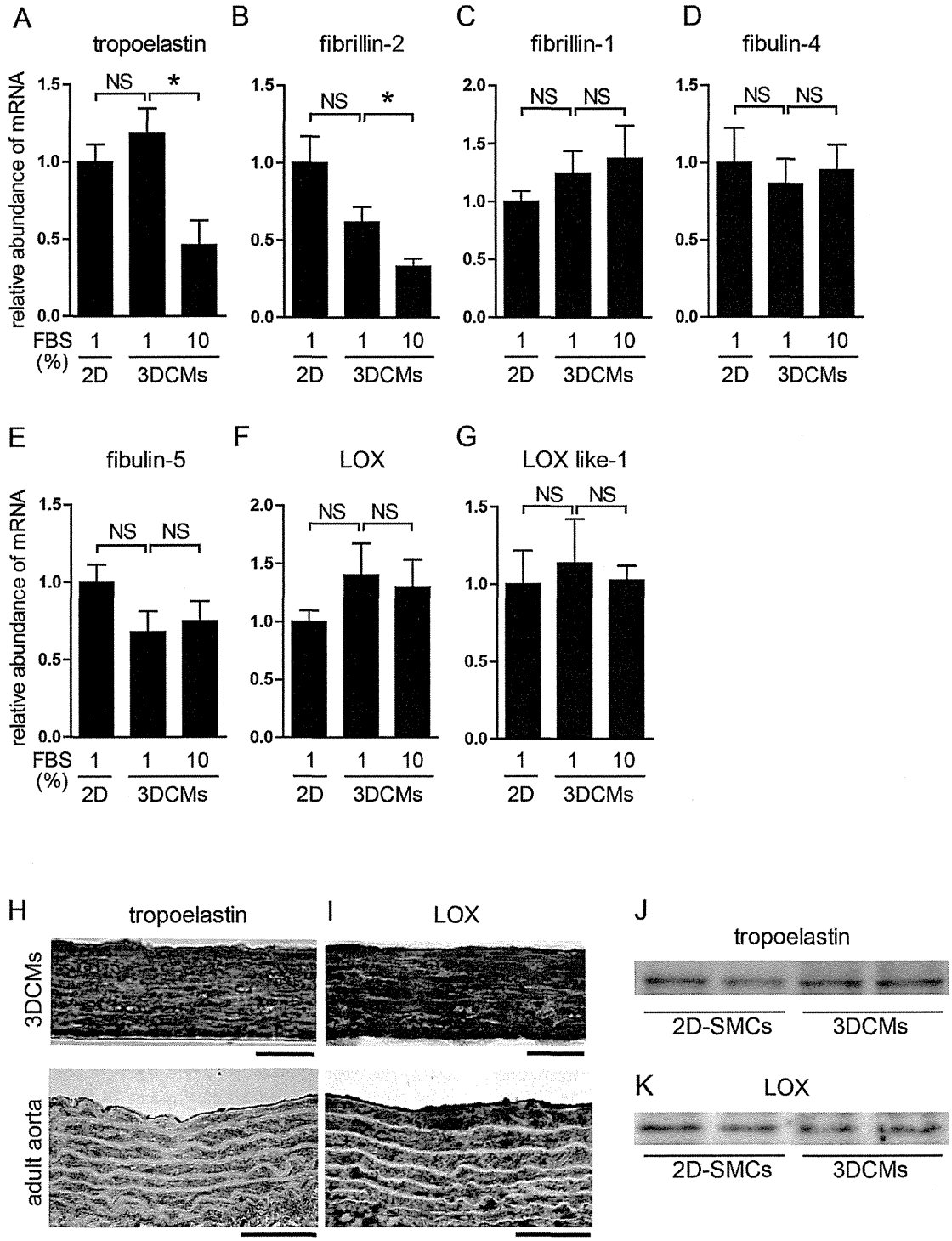

Fig. 2. Expressions of elastic fiber–related genes in 3DCMs. (A–G) Expressions of tropoelastin (A), fibrillin-2 (B), fibrillin-1 (C), fibulin-4 (D), fibulin-5 (E), LOX (F), and LOX–like 1 (G) mRNA were compared between 2D-SMCs (2D) cultured in 1% FBS/DMEM and 3DCMs cultured either in 1% FBS/DMEM or 10% FBS/DMEM. $n = 6–8$. $^*p < 0.05$. NS: not significant. (H–I) Immunohistochemistry for tropoelastin (H) and LOX (I). Brown color indicates positive staining. top panels: 3DCMs. Scale bars: 10 μm lower panels: rat adult aorta. Scale bars: 50 μm. (J–K) Immunoblot analysis for elastin (J), and LOX (K) in 2D-SMCs and 3DCMs.

suggest that the 3D-SMC arrangement per se did not affect elastic fiber–related gene expressions, and that the serum withdrawal likely induced an enhancement of the expression of tropoelastin and fibrillin-2, resulting in elastic fiber formation in the 3DCMs cultured in 1% FBS/DMEM.

3.3. Characterization of the SMC phenotype in 3DCMs

In contrast to the highly differentiated SMCs in mature adult organs, SMCs readily undergo phenotypic changes after isolation and subsequent conventional planar culture [29]. We examined